

Secondary protons from ultra high energy cosmic ray nuclei: is the Greisen-Zatsepin-Kuzmin cutoff unavoidable?

R. Aloisio,¹ V. Berezinsky,¹ and A. Gazizov¹

¹INFN, Laboratori Nazionali del Gran Sasso, I-67010 Assergi (AQ), Italy

We discuss production of ultra high energy secondary protons by cosmic ray primary nuclei propagating in intergalactic space through Cosmic Microwave Background (CMB) and infrared (IR) radiations. Under assumption that only primary nuclei with fixed atomic mass number A_0 are accelerated, the spectrum of secondary protons is calculated. It is found that for all A_0 the diffuse flux of secondary protons starts to dominate over that of primary nuclei at energy $E \sim (1-2) \times 10^{19}$ eV, and thus the standard Greisen-Zatsepin-Kuzmin (GZK) cutoff is produced.

PACS numbers: 98.70 Sa, 13.85.Tp

Ultra High Energy Cosmic Ray (UHECR) puzzle is one of the oldest puzzles in physics, which exists for more than 40 years and most probably now is close to being resolved. It appeared in 1966 together with prediction of the Greisen-Zatsepin-Kuzmin (GZK) cutoff [1]. As physical phenomenon the GZK cutoff is explained by production of pions by UHE extragalactic protons interacting with CMB photons. In the diffuse spectrum the GZK feature (steepening of the spectrum) starts at energy $(3-5) \times 10^{19}$ eV. The UHECR puzzle was born simultaneously with prediction of the GZK feature, because already in 1966 there were known at least three events with energies above the GZK cutoff. With time the number of these events increased and in 2004 there were known at least 16 events with energies higher than 1×10^{20} eV, much above the beginning of GZK cutoff. Now there are strong indications that steepening of the spectrum compatible with GZK cutoff is observed by two detectors, HiRes and Pierre Auger Observatory (PAO). The observation of the GZK feature in differential spectrum measured by HiRes [2] is confirmed by the measured value of $E_{1/2} = 5.3 \times 10^{19}$ eV in the integral spectrum. $E_{1/2}$ is a model-independent characteristic of the GZK cutoff in the integral spectrum [3, 4], whose predicted value precisely coincides with value measured by HiRes. The Auger (PAO) differential spectrum is also consistent with the GZK steepening [5].

However, below the GZK cutoff the Auger data show the mixed mass composition, much heavier than pure proton composition [5]. If primary particles accelerated at the sources are heavy nuclei, why GZK cutoff, which is a signature of protons, is observed? This problem is further strengthened by the Auger observation of correlation with AGN at energy $E \gtrsim 6 \times 10^{19}$ eV [6], which also requires a proton-dominated composition.

In this paper we demonstrate that the pure nucleus primary component accelerated in sources results in the diffuse spectrum which is strongly dominated by protons at energy above $(2-3) \times 10^{19}$ eV, i.e. at energy just below the beginning of the GZK cutoff. This proton component is produced by photo-disintegration of primary nuclei on CMB.

We follow the paper [7] in analytic calculations of spec-

tra. We consider the expanding universe homogeneously filled by the sources of accelerated primary nuclei A_0 with maximum energy $E_{\max}^{\text{acc}} = Z_0 \times 10^{21}$ eV, where A_0 and Z_0 are atomic mass number and charge number, respectively. The generation rate per unit comoving volume $Q_{A_0}(\Gamma, z)$ is given by

$$Q_{A_0}(\Gamma, z) = \frac{(\gamma_g - 2)}{m_N A_0} \mathcal{L}_0 \Gamma^{-\gamma_g}, \quad (1)$$

where z is redshift, Γ is Lorentz factor of accelerated nucleus, γ_g is the generation index, m_N is a mass of nucleon and \mathcal{L}_0 is emissivity, i.e. energy generated per unit comoving volume and per unit time at $z = 0$. In Eq. (1) we assume $\Gamma_{\min} \sim 1$.

Propagating from a source a primary nucleus A_0 diminishes its Lorentz factor and atomic mass number due to interaction with background radiations, most notably with CMB and infrared (IR). The Lorentz factor changes due to adiabatic ($d\Gamma/dt = -b_{\text{ad}}(z)$) and e^+e^- ($d\Gamma/dt = -b_{\text{pair}}^A(\Gamma, z)$) energy losses and atomic number due to photo-disintegration losses ($dA/dt = -b_{\text{dis}}(A, \Gamma, z)$). An important characteristic of propagation is the mean time of nucleus photo-disintegration $\tau_A = 1/b_{\text{dis}} = (dA/dt)^{-1}$.

We study the nucleus evolution in the backward time, whose role is played by redshift z . We consider as initial state the Lorentz factor Γ at $z_0 = 0$ and calculate $\Gamma(z)$ for the fixed value A using the equation

$$\frac{d\Gamma}{dz} = \left| \frac{dt}{dz} \right| [b_{\text{ad}}(z) + b_{\text{pair}}^A(\Gamma, z)], \quad (2)$$

where $dt/dz = -1/[(1+z)H(z)]$ and the Hubble parameter at redshift z is $H(z) = H_0 \sqrt{(1+z)^3 \Omega_m + \Omega_\Lambda}$ with Ω_m and Ω_Λ being relative cosmological matter density and vacuum energy density, respectively. The numerical solution of Eq. (2) gives the evolution trajectory

$$\Gamma_g(z) = G_A(\Gamma, z_0, z), \quad (3)$$

where the first two arguments describe the initial conditions.

The space density of species a can be found from ki-

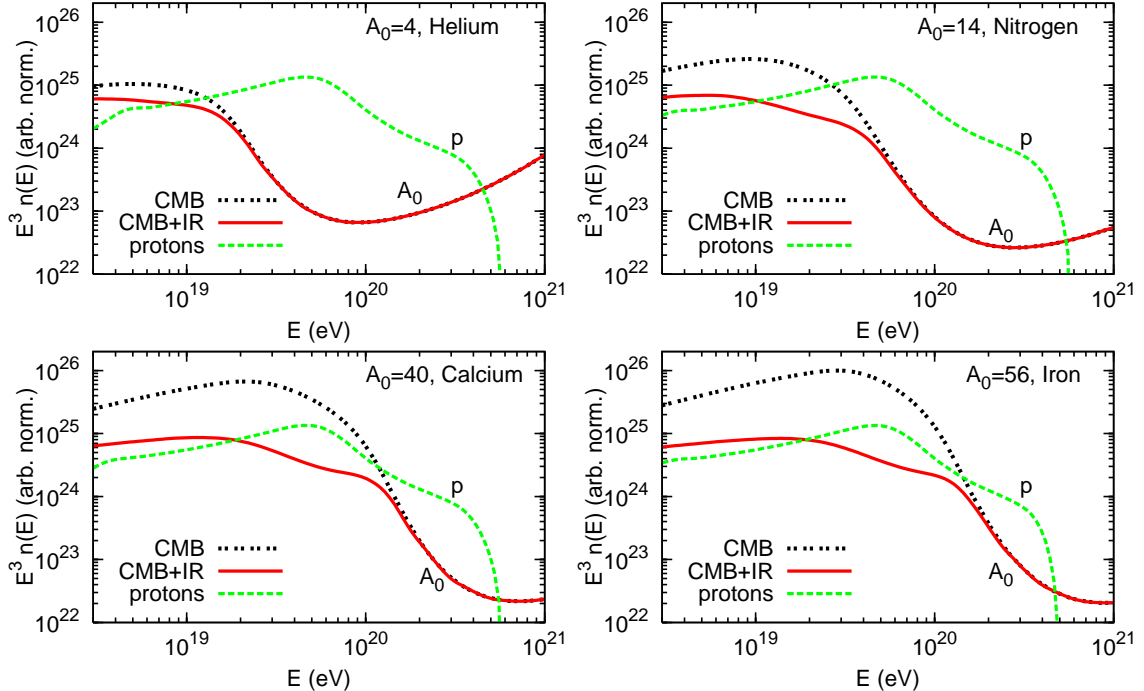


FIG. 1: Flux of primary nuclei A_0 interacting only with CMB (black dotted curves labelled by “ A_0 ”) and with interaction with IR included (red solid curves labelled by A_0) in comparison with secondary proton flux (green dashed curves labeled by “ p ”) for different values of A_0 and for $\gamma_g = 2.3$. In case of CMB+IR the secondary protons start to dominate at energy $(1-2) \times 10^{19}$ eV.

netic equation

$$\frac{\partial}{\partial t} n_a(\Gamma, t) - \frac{\partial}{\partial \Gamma} [b_a(\Gamma, t) n_a(\Gamma, t)] + \frac{n_a(\Gamma, t)}{\tau_a(\Gamma, t)} = Q_a(\Gamma, t). \quad (4)$$

The solution of Eq. (4) for primary nuclei ($a = A_0$) accelerated at the source reads

$$n_{A_0}(\Gamma) = \int_0^\infty dz_g \left| \frac{dt_g}{dz_g} \right| Q_{A_0}(\Gamma_g, z_g) \frac{d\Gamma_g}{d\Gamma} e^{-\eta(\Gamma_g, z_g)}, \quad (5)$$

where Γ_g is given by the evolution function (3), the generation function - by Eq. (1) and analytic expression for $d\Gamma_g/d\Gamma$ is given in [7]. The quantity η takes into account the photo-disintegration of the propagating nucleus:

$$\eta(\Gamma_g, z_g) = \int_{t(z_g)}^{t_0} \frac{dt}{\tau_{A_0}(\Gamma(t), t)}. \quad (6)$$

The lower limit of integration in Eq. (5) reflects the assumption of homogeneous distribution of the sources. The upper limit is imposed by factor $\exp(-\eta)$ accompanied by condition of maximum acceleration Lorentz factor: $Q_{A_0}(\Gamma_g) = 0$, if $\Gamma_g \geq \Gamma_{\max}^{\text{acc}}$.

Secondary protons are produced in the photo-disintegration chain of the primary nucleus A_0 in the processes $\gamma + A \rightarrow (A-1) + N$, where γ is a background photon and N is a nucleon. The total flux of secondary protons is found in [7] through the computation

scheme in which the secondary protons from all intermediate nuclei with $A < A_0$ are taken into account. Another (approximate) method developed there is based on assumption of *instantaneous* decay (photo-disintegration) of primary nuclei to A_0 nucleons. Numerical computations have shown that fluxes calculated by both methods coincide with very good accuracy. We use here the more simple method of instantaneous decay.

Every primary nucleus emitted by a source is considered as A_0 protons and the solution of Eq. (4) for $a = p$ with $\tau_p = \infty$ reads

$$n_p^{\text{inst}}(\Gamma) = A_0 \int_{z_g^{\min}(A_0)}^{z_g^{\max}} dz_g \left| \frac{dt_g}{dz_g} \right| Q_{A_0}(\Gamma_g^p, z_g) \frac{d\Gamma_g^p}{d\Gamma}, \quad (7)$$

where $\Gamma_g^p(z_g)$ is the Lorentz factor of a proton at generation, i.e. $\Gamma_g^p(z_g) = G_p(\Gamma, z_0, z_g)$, and ratio $d\Gamma_g^p/d\Gamma$ is given in [4, 7]. The term $e^{-\eta}$ in Eq. (7) is absent because $\tau_p = \infty$. Since $Q_{A_0} \propto 1/A_0$ (see Eq. 1), the factor A_0 disappears from Eq. (7), and the flux of secondary protons is universal, i.e. the same for all A_0 [7].

The calculated diffuse spectra of primary nuclei and secondary protons are displayed in Fig. 1 for different A_0 , for $\gamma_g = 2.3$ and for the cases of CMB only and CMB+IR with IR/optical flux taken from [8]. The transition from primary nuclei to secondary protons occurs at energies $(1-2) \times 10^{19}$ eV for different A_0 . The physics of this transition is based on universality of secondary-

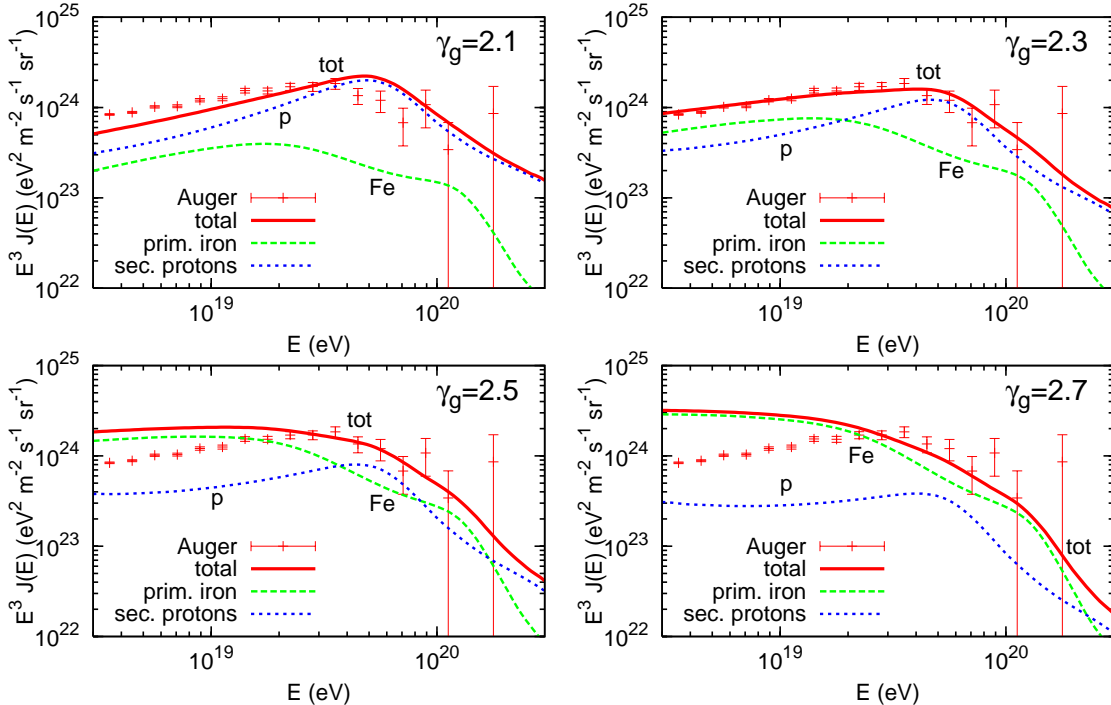


FIG. 2: Flux of primary iron nuclei (green dashed lines labelled by “Fe”) and secondary protons (blue dashed lines labelled by “p”) for different generation indices γ_g . The total spectrum (sum of primary iron and secondary protons) are shown by full red line and compared with the Auger surface detector spectrum. The energy of intersection of iron and secondary proton spectra increases with γ_g .

proton spectrum. In the energy range displayed in Fig. 1, this spectrum is produced by photo-disintegration of nuclei on CMB, and the secondary-proton flux is the same with good accuracy in all four panels. The photo-disintegration of nuclei at energy $E_A \sim 10^{19}$ eV is dominated by IR/optical radiation, while the produced secondary protons have energies $E_p \sim E_A/A$, much below, in case of large A , the discussed transition. Therefore, increasing the IR flux results in suppression of primary-nucleus spectrum without changing the secondary-proton spectrum at energies of interest. It lowers the energy of transition. Fig. 2 demonstrates the dependence of transition energy on generation index γ_g and gives comparison of energy spectrum with Auger observations [9]. The calculations are performed for four values of γ_g . One may observe that with increasing γ_g from 2.1 to 2.7 the energy of transition increases. This effect is easy to understand. Let us consider the unmodified spectrum of primary nuclei A_0 and secondary protons in the toy model, where Lorentz factor is conserved, and photo-disintegration to A_0 nucleons due to interaction with CMB is instantaneous. The ratio of the secondary proton spectrum and unmodified nucleus spectrum in terms of Lorentz factor is $n_p(\Gamma)/n_A^{\text{unm}}(\Gamma) = A_0$. From this ratio it is easy to obtain the ratio for equal energy fluxes $n_p(E)/n_A^{\text{unm}}(E) = A_0^{2-\gamma_g}$. This ratio is suppressed by large γ_g and this suppression survives after the flux of

primaries is reduced by photo-disintegration on IR radiation. This mechanism predicts that dependence of transition energy on γ_g is weaker for the light primaries and numerical calculations confirm it.

Fig. 2 shows that agreement with Auger spectrum is much better for the flat generation spectra with $\gamma_g = 2.1-2.3$ than for the steep spectra. The transition energy for $\gamma_g \leq 2.3$ is less than 2×10^{19} eV.

The generation spectra with $\gamma_g > 2.3$ are disfavored by the observed spectrum, though it is allowed theoretically in the shock acceleration [10]: the distribution of the sources over maximum energy of acceleration $E_{\text{max}}^{\text{acc}}$ or over luminosities makes the effective generation spectrum steeper at the highest energies.

Secondary-proton dominance depends on IR flux, which suppresses the primary-nucleus flux. We shall demonstrate here that if IR flux measured at the present epoch $z = 0$ is correct, the energy of transition remains the same or shifts (in case of strong evolution of the sources) to the lower energies. We are interested thus in the minimum IR flux at $z > 0$. We can prove the following general statement, valid for any diffuse background radiation:

In the case of the generation rate of background radiation $Q(\epsilon, z) = K\epsilon^{-\alpha}(1+z)^m$, valid up to z_{max} , with arbitrary α , $m \geq 0$ and z_{max} , and under the assumption that the background photons are not absorbed, the

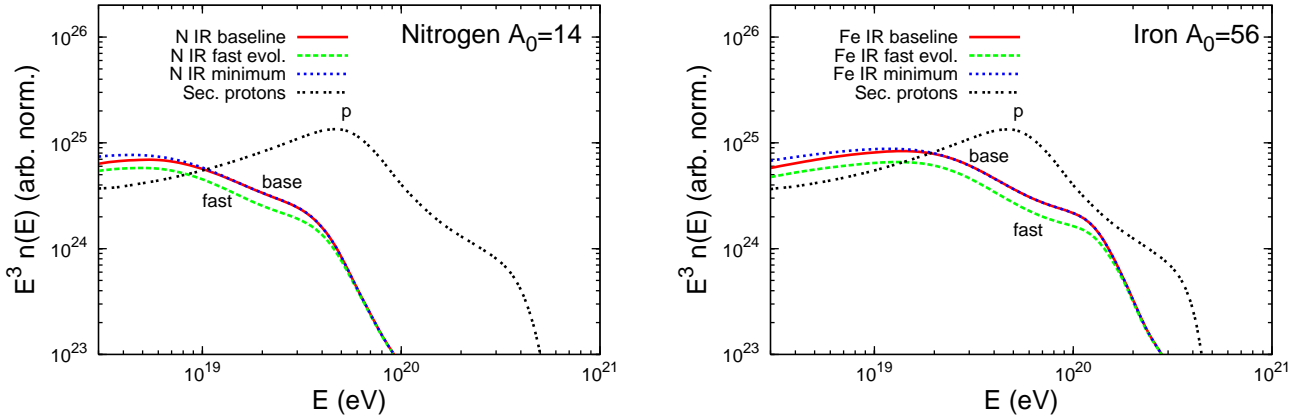


FIG. 3: The influence of IR/optical flux at epoch z on energy of transition. The spectra of primary nuclei are displayed for three IR fluxes, which are the same at $z = 0$, but differ at $z > 0$. The standard one [8] shown by red solid curve labelled by “base”, the larger flux with fast evolution [8] is shown by green dashed line and labelled by “fast” and the absolute minimum of the flux at redshift z is shown by blue dotted line (it practically coincide with the baseline curve). The transition energy is given by intersection of proton flux (black dotted line) with one of the primary-nucleus curves. For minimum IR flux the energy of transition is the same as for the standard IR flux.

flux of diffuse background radiation at epoch z cannot be lower than $J_z(\epsilon) = (1+z)^{-3/2} J_0(\epsilon)$, where $J_0(\epsilon)$ is the flux measured at $z = 0$.

In Fig. 3 we illustrate the effect of variation of the space density of IR photons $n_{\text{IR}}(\epsilon, z)$ with redshift z . Three models of IR fluxes are used for calculations of the flux of UHE primary nuclei: the baseline model of Ref. [8], which is considered as the standard model, the fast evolution model of Ref. [8], which gives the larger IR flux at higher z , and the absolute lower limit for the IR flux at epoch z as given above. The case of the minimum IR flux is very close to the standard one and does not change our conclusions. It is explained by the fact that the fluxes of UHE nuclei at $E > 1 \times 10^{19}$ eV are produced at very small z and thus interact practically with $z = 0$ flux of IR radiation, when the source evolution is weak.

In conclusion, the preferential acceleration of heavy nuclei in the sources is naturally accompanied by dominance of the protons in the diffuse spectrum at energy higher than $(1-2) \times 10^{19}$ eV with the standard GZK cut-

off. We studied the extreme case of nuclei acceleration solely, and found the dominance of secondary protons. In shock acceleration some fraction of accelerated protons is unavoidably present, and this primary component strengthens further the proton dominance [11]. Another effect which increases the proton dominance is diffusion. The diffusion coefficient is inversely proportional to the charge number Z and thus time of nuclei propagation from nearby sources becomes longer and nuclei are destroyed. Variation of IR flux with z also cannot increase the transition energy. The only effect which increases the transition energy is the large effective generation index of UHE nuclei $\gamma_g > 2.3$. We conclude that the GZK cutoff in the observational data is compatible with heavy mass composition below the GZK cutoff in all most reasonable cases.

We are grateful to Floyd Stecker for helpful correspondence. This work is partially funded by the contract ASI-INAF I/088/06/0 for theoretical studies in High Energy Astrophysics.

[1] K. Greisen, Phys. Rev. Lett. **16**, 748 (1966); G. T. Zatsepin, V. A. Kuzmin, Pisma Zh. Experim. Theor. Phys. **4**, 114 (1966).
[2] R. U. Abbasi [HiRes collaboration], astro-ph/0707.2638.
[3] V. S. Berezinsky and S. I. Grigorieva, Astron. Astrophys. **199**, 1 (1988).
[4] V. Berezinsky, A. Gazizov and S. Grigorieva, Phys. Rev. D **74**, 043005 (2006) (see also hep-ph/0204357v1).
[5] A. A. Watson, Highlight talk at 30th ICRC conference (Merida, Mexico 2007), arXiv:0801.4050.
[6] The Pierre Auger Collaboration. arXiv:0711.2256.
[7] R. Aloisio, V. Berezinsky, S. Grigoieva, arXiv:0802.4452.
[8] F. W. Stecker, M. A. Malkan, S. T. Scully, Astroph. J **648**, 774 (2006).
[9] T. Yamamoto (Pierre Auger Collaboration), 30th ICRC conference (Merida, Mexico 2007), arXiv:0707.2638.
[10] M. Kachelriess and D. Semikoz, Phys. Lett. B **634**, 143 (2006); R. Aloisio et al, Astropart. Phys. **27**, 76 (2007).
[11] D. Allard, A. Olinto, E. Parizot, astro-ph/0703633.